

The Properties of Compressible MHD and Cosmic Ray Transport

A. Lazarian, Jungyeon Cho, & Huirong Yan

Dept. of Astronomy, Univ. of Wisconsin, Madison WI53706, USA

ABSTRACT

Turbulence is the most common state of astrophysical flows. In typical astrophysical fluids, turbulence is accompanied by strong magnetic fields, which has a large impact on the dynamics of the turbulent cascade. Recently, there has been a significant breakthrough on the theory of magnetohydrodynamic (MHD) turbulence. For the first time we have a scaling model that is supported by both observations and numerical simulations. We review recent progress in studies of both incompressible and compressible turbulence. We compare Iroshnikov-Kraichnan and Goldreich-Sridhar models, and discuss scalings of Alfvén, slow, and fast waves. We discuss the implications of this new insight into MHD turbulence for cosmic ray transport.

1. Introduction

Most astrophysical systems, e.g. accretion disks, stellar winds, the interstellar medium (ISM) and intercluster medium are turbulent with an embedded magnetic field that influences almost all of their properties. This turbulence which spans from km to many kpc (see discussion in Armstrong, Rickett, & Spangler 1995; Scalo 1987; Lazarian, Pogosyan, & Esquivel 2002) holds the key to many astrophysical processes. For instance, propagation of cosmic rays and their acceleration is strongly affected by MHD turbulence. Recent research has shown that a substantial part of the earlier results in the field require revision. Earlier research used ad hoc models of MHD turbulence and this entailed erroneous conclusions.

Before we start a discussion of MHD turbulence let us recall some basic properties of the hydrodynamic turbulence. All turbulent systems have one thing in common: they have a large “Reynolds number” ($Re \equiv LV/\nu$; L = the characteristic scale or driving scale of the system, V =the velocity difference over this scale, and ν =viscosity), the ratio of the viscous drag time on the largest scales (L^2/ν) to the eddy turnover time of a parcel of gas (L/V). A similar parameter, the “magnetic Reynolds number”, $Rm \equiv LV/\eta$; η =magnetic diffusion), is the ratio of the magnetic field decay time (L^2/η) to the eddy turnover time (L/V). The properties of the flows on all scales depend on Re and Rm . Flows with $Re < 100$ are laminar; chaotic structures develop gradually as Re increases, and those with $Re \sim 10^3$ are appreciably less chaotic than those with $Re \sim 10^7$. Observed features such as star forming clouds and accretion disks are very chaotic with $Re > 10^8$ and $Rm > 10^{16}$.

Let us start by considering incompressible hydrodynamic turbulence, which can be described by the Kolmogorov theory (Kolmogorov 1941). Suppose that we excite fluid motions at a scale L . We call this scale the *energy injection scale* or the *largest energy containing eddy scale*. For instance, an obstacle in a flow excites motions on scales of the order of its size. Then the energy injected at the scale L cascades to progressively smaller and smaller scales at the eddy turnover rate, i.e. $\tau_l^{-1} \approx v_l/l$, with negligible energy losses along the cascade¹. Ultimately, the energy reaches the molecular dissipation scale l_d , i.e. the scale where the local $Re \sim 1$, and is dissipated there. The scales between L and l_d are called the *inertial range* and it typically covers many decades. The motions over the inertial range are *self-similar* and this provides tremendous advantages for theoretical description.

The beauty of the Kolmogorov theory is that it does provide a simple scaling for hydrodynamic motions. If the velocity at a scale l from the inertial range is v_l , the Kolmogorov theory states that the kinetic energy ($\rho v_l^2 \sim v_l^2$ as the density is constant) is transferred to next scale within one eddy turnover time (l/v_l). Thus within the Kolmogorov theory the energy transfer rate ($v_l^2/(l/v_l)$) is scale-independent,

$$\frac{v_l^2}{t_{cas}} \sim \frac{v_l^2}{(l/v_l)} = \text{constant}, \quad (1)$$

and we get the famous Kolmogorov scaling

$$v_l \propto l^{1/3}. \quad (2)$$

The one-dimensional² energy spectrum $E(k)$ is the amount of energy between the wavenumber k and $k + dk$ divided by dk . When $E(k)$ is a power law, $kE(k)$ is the energy *near* the wavenumber $k \sim 1/l$. Since $v_l^2 \approx kE(k)$, Kolmogorov scaling implies

$$E(k) \propto k^{-5/3}. \quad (3)$$

Kolmogorov scalings were the first major advance in the theory of incompressible turbulence. They have led to numerous applications in different branches of science (see Monin & Yaglom 1975). However, astrophysical fluids are magnetized and the a dynamically important magnetic field should interfere with eddy motions.

Paradoxically, astrophysical measurements are consistent with Kolmogorov spectra (see LPE02). For instance, interstellar scintillation observations indicate an electron density spectrum is very close to $-5/3$ for $10^8 \text{ cm} - 10^{15} \text{ cm}$ (see Armstrong et al. 1995). At larger scales LPE02 summarizes the evidence of $-5/3$ velocity power spectrum over pc-scales in HI. Solar-wind observations provide *in-situ* measurements of the power spectrum of magnetic fluctuations and Leamon et al. (1998) also

¹This is easy to see as the motions at the scales of large eddies have $Re \gg 1$.

²Dealing with observational data, e.g. in LPE02 (Lazarian et al. 2002), we deal with three dimensional energy spectrum $P(k)$, which, for isotropic turbulence, is given by $E(k) = 4\pi k^2 P(k)$.

obtained a slope of $\approx -5/3$. Is this a coincidence? What properties is the magnetized compressible ISM expected to have? We will deal with these questions, and some related issues, below.

Here we discuss a focused approach which aims at obtaining a clear understanding on the fundamental level, and considering physically relevant complications later. The creative synthesis of both approaches is the way, we think, that studies of astrophysical turbulence should proceed³. Certainly an understanding of MHD turbulence in the most ideal terms is a necessary precursor to understanding the complications posed by more realistic physics and numerical effects. For review of general properties of MHD, see a recent book by Biskamp (1993).

In what follows, we first consider observational data that motivate our study (§2), then discuss theoretical approaches to incompressible MHD turbulence (§3). We move to the effects of compressibility in §4 and discuss implications of our new understanding of MHD turbulence for cosmic ray dynamics in §5. We present the summary in §6.

2. Observational Data

Kolmogorov turbulence is the simplest possible model of turbulence. Since it is incompressible and not magnetized, it is completely specified by its velocity spectrum. If a passive scalar field, like “dye particles” or temperature inhomogeneities, is subjected to Kolmogorov turbulence, the resulting spectrum of the passive scalar density is also Kolmogorov (see Lesieur 1990; Warhaft 2000). In compressible and magnetized turbulence this is no longer true, and a complete characterization of the turbulence requires not only a study of the velocity statistics but also the statistics of density and magnetic fluctuations.

Direct studies of turbulence⁴ have been done mostly for interstellar medium and for the Solar wind. While for the Solar wind *in-situ* measurements are possible, studies of interstellar turbulence require inverse techniques to interpret the observational data.

Attempts to study interstellar turbulence with statistical tools date as far back as the 1950s (von Horner 1951; Kampé de Fériet 1955; Munch 1958; Wilson et al. 1959) and various directions of research achieved various degree of success (see reviews by Kaplan & Pickelner 1970; Dickman 1985; Armstrong et al. 1995; Lazarian 1999a, 1999b; LPE02).

³Potentially our approach leads to an understanding of the relationship between motions at a given time at small scales (subgrid scales) and the state of the flow at a previous time at some larger, resolved, scale. This could lead to a parametrization of the subgrid scales and to large eddy simulations of MHD.

⁴Indirect studies include the line-velocity relationships (Larson 1981) where the integrated velocity profiles are interpreted as the consequence of turbulence. Such studies do not provide the statistics of turbulence and their interpretation is very model dependent.

2.1. Solar wind

Solar wind (see review Goldstein & Roberts 1995) studies allow pointwise statistics to be measured directly using spacecrafts. These studies are the closest counterpart of laboratory measurements.

The solar wind flows nearly radially away from the Sun, at up to about 700 km/s. This is much faster than both spacecraft motions and the Alfvén speed. Therefore, the turbulence is “frozen” and the fluctuations at frequency f are directly related to fluctuations at the scale k in the direction of the wind, as $k = 2\pi f/v$, where v is the solar wind velocity (Horbury 1999).

Usually two types of solar wind are distinguished, one being the fast wind which originates in coronal holes, and the slower bursty wind. Both of them show, however, $f^{-5/3}$ scaling on small scales. The turbulence is strongly anisotropic (see Klein et al. 1993) with the ratio of power in motions perpendicular to the magnetic field to those parallel to the magnetic field being around 30. The intermittency of the solar wind turbulence is very similar to the intermittency observed in hydrodynamic flows (Horbury & Balogh 1997).

2.2. Electron density statistics

Studies of turbulence statistics of ionized media (see Spangler & Gwinn 1990) have provided information on the statistics of plasma density at scales 10^8 - 10^{15} cm. This was based on a clear understanding of processes of scintillations and scattering achieved by theorists⁵ (see Narayan & Goodman 1989; Goodman & Narayan 1985). A peculiar feature of the measured spectrum (see Armstrong et al. 1995) is the absence of the slope change at the scale at which the viscosity by neutrals becomes important.

Scintillation measurements are the most reliable data in the “big power law” plot in Armstrong et al. (1995). However there are intrinsic limitations to the scintillations technique due to the limited number of sampling directions, its relevance only to ionized gas at extremely small scales, and the impossibility of getting velocity (the most important!) statistics directly. Therefore with the data one faces the problem of distinguishing actual turbulence from static density structures. Moreover, the scintillation data does not provide the index of turbulence directly, but only shows that the data are consistent with Kolmogorov turbulence. Whether the (3D) index can be -4 instead of -11/3 is still a subject of intense debate (Higdon 1984; Narayan & Goodman 1989). In physical terms the former corresponds to the superposition of random shocks rather than eddies.

Additional information on the electron density is contained in the Faraday rotation measures of extragalactic radio sources (see Simonetti & Cordes 1988; Simonetti 1992). However, there is so far no reliable way to disentangle contributions of the magnetic field and the density to the

⁵In fact, the theory of scintillations was developed first for the atmospheric applications.

signal. We feel that those measurements may give us the magnetic field statistics when we know the statistics of electron density better.

2.3. Velocity and density statistics from spectral lines

Spectral line data cubes are unique sources of information on interstellar turbulence. Doppler shifts due to supersonic motions contain information on the turbulent velocity field which is otherwise difficult to obtain. Moreover, the statistical samples are extremely rich and not limited to discrete directions. In addition, line emission allows us to study turbulence at large scales, comparable to the scales of star formation and energy injection.

However, the problem of separating velocity and density fluctuations within HI data cubes is far from trivial (Lazarian 1995, 1999b; Lazarian & Pogosyan 2000; LPE02). The analytical description of the emissivity statistics of channel maps (velocity slices) in Lazarian & Pogosyan (2000) (see also Lazarian 1999b; LPE02 for reviews) shows that the relative contribution of the density and velocity fluctuations depends on the thickness of the velocity slice. In particular, the power-law asymptote of the emissivity fluctuations changes when the dispersion of the velocity at the scale under study becomes of the order of the velocity slice thickness (the integrated width of the channel map). These results are the foundation of the Velocity-Channel Analysis (VCA) technique which provides velocity and density statistics using spectral line data cubes. The VCA has been successfully tested using data cubes obtained via compressible magnetohydrodynamic simulations and has been applied to Galactic and Small Magellanic Cloud atomic hydrogen (HI) data (Lazarian et al. 2001; Lazarian & Pogosyan 2000; Stanimirovic & Lazarian 2001; Deshpande, Dwarakanath, & Goss 2000). Furthermore, the inclusion of absorption effects (Lazarian & Pogosyan 2002) has increased the power of this technique. Finally, the VCA can be applied to different species (CO, H α etc.) which should further increase its utility in the future.

Within the present discussion a number of results obtained with the VCA are important. First of all, the Small Magellanic Cloud (SMC) HI data exhibit a Kolmogorov-type spectrum for velocity and HI density from the smallest resolvable scale of 40 pc to the scale of the SMC itself, i.e. 4 kpc. Similar conclusions can be inferred from the Galactic data (Green 1993) for scales of dozens of parsecs, although the analysis has not been done systematically. Deshpande et al. (2000) studied absorption of HI on small scales toward Cas A and Cygnus A. Within the VCA their results can be interpreted as implying that on scales less than 1 pc the HI velocity is suppressed by ambipolar drag and the spectrum of density fluctuations is shallow $P(k) \sim k^{-2.8}$. Such a spectrum (Deshpande 2000) can account for the small scale structure of HI observed in absorption.

2.4. Magnetic field statistics

Magnetic field statistics are the most poorly constrained aspect of ISM turbulence. The polarization of starlight and of the Far-Infrared Radiation (FIR) from aligned dust grains is affected by the ambient magnetic fields. Assuming that dust grains are always aligned with their longer axes perpendicular to magnetic field (see the review Lazarian 2000), one gets the 2D distribution of the magnetic field directions in the sky. Note that the alignment is a highly non-linear process in terms of the magnetic field and therefore the magnetic field strength is not available⁶.

The statistics of starlight polarization (see Fosalba et al. 2002) is rather rich for the Galactic plane and it allows to establish the spectrum⁷ $E(K) \sim K^{-1.5}$, where K is a two dimensional wave vector describing the fluctuations over sky patch.⁸ For uniformly sampled turbulence it follows from Lazarian & Shutenkov (1990) that $E(K) \sim K^\alpha$ for $K < K_0$ and K^{-1} for $K > K_0$, where K_0^{-1} is the critical angular size of fluctuations which is proportional to the ratio of the injection energy scale to the size of the turbulent system along the line of sight. For Kolmogorov turbulence $\alpha = -11/3$.

However, the real observations do not uniformly sample turbulence. Many more close stars are present compared to the distant ones. Thus the intermediate slopes are expected. Indeed, Cho & Lazarian (2002b) showed through direct simulations that the slope obtained in Fosalba et al. (2002) is compatible with the underlying Kolmogorov turbulence. At the moment FIR polarimetry does not provide maps that are really suitable to study turbulence statistics. This should change soon when polarimetry becomes possible using the airborne SOFIA observatory. A better understanding of grain alignment (see Lazarian 2000) is required to interpret the molecular cloud magnetic data where some of the dust is known not to be aligned (see Lazarian, Goodman, & Myers 1997 and references therein).

Another way to get magnetic field statistics is to use synchrotron emission. Both polarization and intensity data can be used. The angular correlation of polarization data (Baccigalupi et al. 2001) shows the power-law spectrum $K^{-1.8}$ and we believe that the interpretation of it is similar to that of starlight polarization. Indeed, Faraday depolarization limits the depth of the sampled region. The intensity fluctuations were studied in Lazarian & Shutenkov (1990) with rather poor initial data and the results were inconclusive. Cho & Lazarian (2002b) interpreted the fluctuations of synchrotron emissivity (Giardino et al. 2001, 2002) in terms of turbulence with Kolmogorov spectrum.

⁶The exception to this may be the alignment of small grains which can be revealed by microwave and UV polarimetry (Lazarian 2000).

⁷Earlier papers dealt with much poorer samples (see Kaplan & Pickelner 1970) and they did not reveal power-law spectra.

⁸This spectrum is obtained by Fosalba et al. (2002) in terms of the expansion over the spherical harmonic basis Y_{lm} . For sufficiently small areas of the sky analyzed the multipole analysis results coincide with the Fourier analysis.

3. Theoretical Approaches to MHD Turbulence

Attempts to describe magnetic turbulence statistics were made by Iroshnikov (1963) and Kraichnan (1965). Their model of turbulence (IK theory) is isotropic in spite of the presence of the magnetic field.

For simplicity, let us suppose that a uniform external magnetic field (\mathbf{B}_0) is present. In the incompressible limit, any magnetic perturbation propagates *along* the magnetic field line. Since wave packets are moving along the magnetic field line, there are two possible directions for propagation. If all the wave packets are moving in one direction, then they are stable to nonlinear order (Parker 1979). Therefore, in order to initiate turbulence, there must be opposite-traveling wave packets and the energy cascade occurs only when they collide. The IK theory starts from this observation, one of the consequences of which is the modification of the energy cascade timescale: $t_{cas} \sim (L/V)(V_A/V)$, where $V_A = B_0/\sqrt{4\pi\rho}$ is Alfvén velocity of the mean field. Here, the IK theory assumes that opposite-traveling isotropic wave packets of similar size interact. From this and the scale-invariance of energy cascade rate, they obtained

$$\text{Iroshnikov-Kraichnan: } E(k) \propto k^{-3/2}. \quad (4)$$

However, the presence of the uniform magnetic component has non-trivial dynamical effects on the turbulence fluctuations. One obvious effect is that it is easy to mix field lines in directions perpendicular to the local mean magnetic field and much more difficult to bend them. The IK theory assumes isotropy of the energy cascade in Fourier space, an assumption which has attracted severe criticism (Montgomery & Turner 1981; Shebalin, Matthaeus, & Montgomery 1983; Montgomery & Matthaeus 1995; Sridhar & Goldreich 1994; Matthaeus et al. 1998). Mathematically, anisotropy manifests itself in the resonant conditions for 3-wave interactions:

$$\mathbf{k}_1 + \mathbf{k}_2 = \mathbf{k}_3, \quad (5)$$

$$\omega_1 + \omega_2 = \omega_3, \quad (6)$$

where \mathbf{k} 's are wavevectors and ω 's are wave frequencies. The first condition is a statement of wave momentum conservation and the second is a statement of energy conservation. Alfvén waves satisfy the dispersion relation: $\omega = V_A|k_{\parallel}|$, where k_{\parallel} is the component of wavevector parallel to the background magnetic field. Since only opposite-traveling wave packets interact, \mathbf{k}_1 and \mathbf{k}_2 must have opposite signs. Then from equations (5) and (6), either $k_{\parallel,1}$ or $k_{\parallel,2}$ must be equal to 0 and $k_{\parallel,3}$ must be equal to the nonzero initial parallel wavenumber. That is, zero frequency modes are essential for energy transfer (Shebalin et al. 1983). Therefore, in the wavevector space, 3-wave interactions produce an energy cascade which is strictly perpendicular to the mean magnetic field. However, in real turbulence, equation (6) does not need to be satisfied exactly, but only to within an error of order $\delta\omega \sim 1/t_{cas}$ (Goldreich & Sridhar 1995). This implies that the energy cascade is not strictly perpendicular to \mathbf{B}_0 , although clearly very anisotropic.

We assume throughout this discussion that the rms turbulent velocity at the energy injection scale is comparable to the Alfvén speed of the mean field and consider only scales below the energy

injection scale. This is called *strong* turbulence regime. Note that, as a consequence, the regime of $B_0 \gg \delta b$ is not considered in this review. However, the regime of $B_0 \ll \delta b$ is still relevant to the strong turbulence regime because scales below the energy equipartition scale is expected to fall in the strong turbulence regime (Cho & Vishniac 2000a).

An ingenious model very similar in its beauty and simplicity to the Kolmogorov model has been proposed by Goldreich & Sridhar (1995; hereinafter GS95) for incompressible strong MHD turbulence. They pointed out that motions perpendicular to the magnetic field lines mix them on a hydrodynamic time scale, i.e. at a rate $t_{cas}^{-1} \approx k_{\perp} v_l$, where k_{\perp} is the wavevector component perpendicular to the local mean magnetic field and $l \sim k^{-1} (\approx k_{\perp}^{-1})$. These mixing motions couple to the wave-like motions parallel to magnetic field giving a *critical balance* condition

$$k_{\parallel} V_A \sim k_{\perp} v_k, \quad (7)$$

where k_{\parallel} is the component of the wavevector parallel to the local magnetic field. When the typical k_{\parallel} on a scale k_{\perp} falls below this limit, the magnetic field tension is too weak to affect the dynamics and the turbulence evolves hydrodynamically, in the direction of increasing isotropy in phase space. This quickly raises the value of k_{\parallel} . In the opposite limit, when k_{\parallel} is large, the magnetic field tension dominates, the error $\delta\omega$ in the matching conditions is reduced, and the nonlinear cascade is largely in the k_{\perp} direction, which restores the critical balance.

If conservation of energy in the turbulent cascade applies locally in phase space then the energy cascade rate (v_l^2/t_{cas}) is constant: $(v_l^2)/(l/v_l) = \text{constant}$. Combining this with the critical balance condition we obtain an anisotropy that increases with decreasing scale

$$k_{\parallel} \propto k_{\perp}^{2/3}, \quad (8)$$

and a Kolmogorov-like spectrum for perpendicular motions

$$v_l \propto l^{1/3}, \text{ or } E(k) \propto k_{\perp}^{-5/3}, \quad (9)$$

which is not surprising since the magnetic field does not influence motions that do not bend it. At the same time, the scale-dependent anisotropy reflects the fact that it is more difficult for the weaker, smaller eddies to bend the magnetic field.

GS95 shows the duality of motions in MHD turbulence. Those perpendicular to the mean magnetic field are essentially eddies, while those parallel to magnetic field are waves. The critical balance condition couples these two types of motions.

Numerical simulations (Cho & Vishniac 2000b; Maron & Goldreich 2001; Cho, Lazarian, & Vishniac 2002) show reasonable agreements with the GS95 model.

4. Compressible Turbulence

For the rest of the review, we consider MHD turbulence of a single conducting fluid. While the GS95 model describes incompressible MHD turbulence well, no universally accepted theory

exists for compressible MHD turbulence despite various attempts (e.g., Higdon 1984). Earlier numerical simulations of compressible MHD turbulence covered a broad range of astrophysical problems, such as the decay of turbulence (e.g. Mac Low 1998; Stone, Ostriker, & Gammie 1998) or turbulent modeling of the ISM (see recent review Vazquez-Semadeni 2002; see also Passot, Pouquet, & Woodward 1988; Vazquez-Semadeni, Passot, & Pouquet 1995; Passot, Vazquez-Semadeni, & Pouquet 1995; Vazquez-Semadeni, Passot, & Pouquet 1996 for earlier pioneering 2D simulations and Ostriker, Gammie, & Stone 1999; Ostriker, Stone, & Gammie 2001; Padoan et al. 2001; Klessen 2001; Boldyrev 2002 for recent 3D simulations). In what follows, we concentrate on the fundamental properties of compressible MHD.

4.1. Alfvén, slow, and fast modes

Let us start by reviewing different MHD waves. In particular, we describe the Fourier space representation of these waves. The real space representation can be found in papers on modern shock-capturing MHD codes (e.g. Brio & Wu 1988; Ryu & Jones 1995). For the sake of simplicity, we consider an isothermal plasma. Figure 1 and Figure 2 give schematics of slow and fast waves. For slow and fast waves, \mathbf{B}_0 , $\mathbf{v}_\mathbf{k}$ ($\propto \xi$), and \mathbf{k} are in the same plane. On the other hand, for Alfvén waves, the velocity of the fluid element $(\mathbf{v}_\mathbf{k})_A$ is orthogonal to the $\mathbf{B}_0 - \mathbf{k}$ plane.

As before, the Alfvén speed is $V_A = B_0/\sqrt{4\pi\rho_0}$, where ρ_0 is the average density. Fast and slow speeds are

$$c_{f,s} = \left[\frac{1}{2} \left\{ a^2 + V_A^2 \pm \sqrt{(a^2 + V_A^2)^2 - 4a^2V_A^2 \cos^2 \theta} \right\} \right]^{1/2}, \quad (10)$$

where θ is the angle between \mathbf{B}_0 and \mathbf{k} . See Table 1 for the definition of other variables. When β ($\beta = P_g/P_B=2a^2/V_A^2$; P_g = gas pressure, P_B = magnetic pressure; hereinafter $\beta = \text{average } \beta \equiv \bar{P}_g/\bar{P}_B$) goes to zero, we have

$$c_f \approx V_A,$$

Table 1: Notations for compressible turbulence

Notation	Meaning
a, c_s, c_f, V_A	sound, slow, fast, and Alfvén speed
$\delta V, (\delta V)_s, (\delta V)_f, (\delta V)_A$	random (rms) velocity Previously we used V for the rms velocity
$v_l, (v_l)_s, (v_l)_f, (v_l)_A$	velocity at scale l
$\mathbf{v}_\mathbf{k}, (\mathbf{v}_\mathbf{k})_s, (\mathbf{v}_\mathbf{k})_f, (\mathbf{v}_\mathbf{k})_A$	velocity vector at wavevector \mathbf{k}
$\hat{\mathbf{B}}_0 (= \hat{\mathbf{k}}_\parallel), \hat{\mathbf{k}}_\perp, \hat{\mathbf{k}}, \hat{\theta}, \dots$	unit vectors
ξ_s, ξ_f	displacement vectors

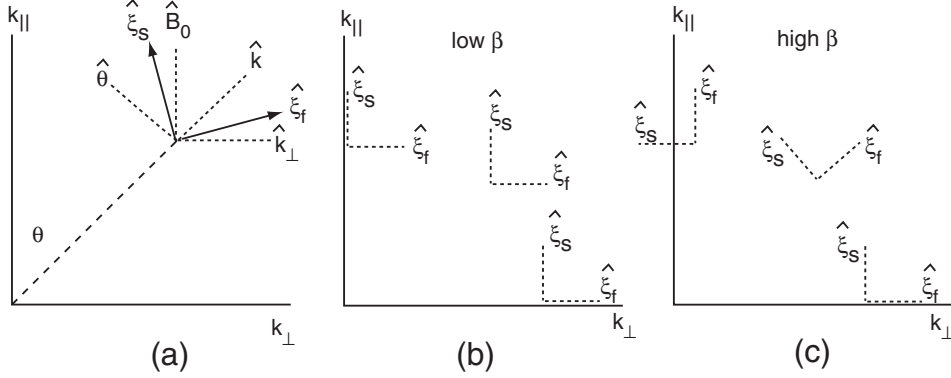


Fig. 1.— (a) Directions of fast and slow basis vectors. $\hat{\boldsymbol{\xi}}_f$ and $\hat{\boldsymbol{\xi}}_s$ represent the directions of displacement of fast and slow modes, respectively. In the fast basis ($\hat{\boldsymbol{\xi}}_f$) is always between $\hat{\mathbf{k}}$ and $\hat{\mathbf{k}}_{\perp}$. In the slow basis ($\hat{\boldsymbol{\xi}}_s$) lies between $\hat{\boldsymbol{\theta}}$ and $\hat{\mathbf{B}}_0$. Here, $\hat{\boldsymbol{\theta}}$ is perpendicular to $\hat{\mathbf{k}}$ and parallel to the wave front. All vectors lie in the same plane formed by \mathbf{B}_0 and \mathbf{k} . On the other hand, the displacement vector for Alfvén waves (not shown) is perpendicular to the plane. (b) Directions of basis vectors for a very small β drawn in the same plane as in (a). The fast bases are almost parallel to $\hat{\mathbf{k}}_{\perp}$. (c) Directions of basis vectors for a very high β . The fast basis vectors are almost parallel to \mathbf{k} . The slow waves become pseudo-Alfvén waves.

$$c_s \approx a \cos \theta. \quad (11)$$

Figure 1 shows directions of displacement (or, directions of velocity) vectors for these three modes. We will call them the basis vectors for these modes. The Alfvén basis is perpendicular to both $\hat{\mathbf{k}}$ and $\hat{\mathbf{B}}_0$, and coincides with the azimuthal vector $\hat{\boldsymbol{\phi}}$ in a spherical-polar coordinate system. Here hatted vectors are unit vectors. The fast basis $\hat{\boldsymbol{\xi}}_f$ lies *between* $\hat{\mathbf{k}}$ and $\hat{\mathbf{k}}_{\perp}$:

$$\hat{\boldsymbol{\xi}}_f \propto \frac{1 - \sqrt{D} + \beta/2}{1 + \sqrt{D} - \beta/2} \left[\frac{k_{\perp}}{k_{\parallel}} \right]^2 k_{\parallel} \hat{\mathbf{k}}_{\parallel} + k_{\perp} \hat{\mathbf{k}}_{\perp}, \quad (12)$$

where $D = (1 + \beta/2)^2 - 2\beta \cos^2 \theta$, and β is the averaged β ($=\bar{P}_g/\bar{P}_B$). The slow basis $\hat{\boldsymbol{\xi}}_s$ lies *between* $\hat{\boldsymbol{\theta}}$ and $\hat{\mathbf{B}}_0$ ($=\hat{\mathbf{k}}_{\parallel}$):

$$\hat{\boldsymbol{\xi}}_s \propto k_{\parallel} \hat{\mathbf{k}}_{\parallel} + \frac{1 - \sqrt{D} - \beta/2}{1 + \sqrt{D} + \beta/2} \left[\frac{k_{\parallel}}{k_{\perp}} \right]^2 k_{\perp} \hat{\mathbf{k}}_{\perp}. \quad (13)$$

The two vectors $\hat{\boldsymbol{\xi}}_f$ and $\hat{\boldsymbol{\xi}}_s$ are mutually orthogonal. Proper normalizations are required for both bases to make them unit-length.

When β goes to zero (i.e. the magnetically dominated regime), $\hat{\boldsymbol{\xi}}_f$ becomes parallel to $\hat{\mathbf{k}}_{\perp}$ and $\hat{\boldsymbol{\xi}}_s$ becomes parallel to $\hat{\mathbf{B}}_0$ (Fig. 1b). The sine of the angle between $\hat{\mathbf{B}}_0$ and $\hat{\boldsymbol{\xi}}_s$ is $(\beta/2) \sin \theta \cos \theta$.

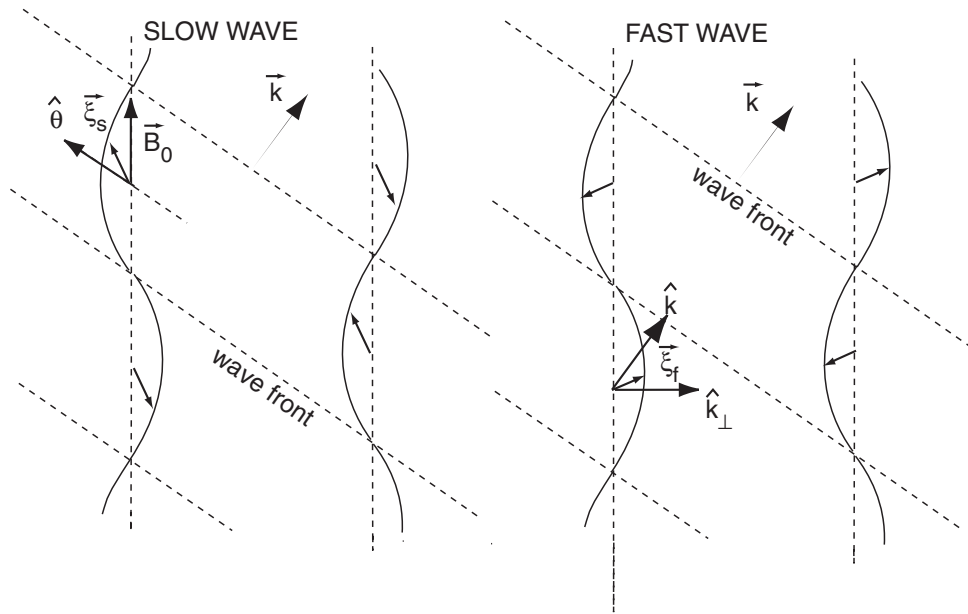


Fig. 2.— Waves in real space. We show the directions of displacement vectors for a slow wave (*left*) and a fast wave (*right*). Note that $\hat{\xi}_s$ lies between $\hat{\theta}$ and $\hat{\mathbf{B}}_0$ ($= \hat{\mathbf{k}}_{\parallel}$) and $\hat{\xi}_f$ between $\hat{\mathbf{k}}$ and $\hat{\mathbf{k}}_{\perp}$. Again, $\hat{\theta}$ is perpendicular to $\hat{\mathbf{k}}$ and parallel to the wave front. Note also that, for the fast wave, for example, density (inferred by the directions of the displacement vectors) becomes higher where field lines are closer, resulting in a strong restoring force, which is why fast waves are faster than slow waves.

When β goes to infinity (i.e. gas pressure dominated regime)⁹, $\hat{\xi}_f$ becomes parallel to $\hat{\mathbf{k}}$ and $\hat{\xi}_s$ becomes parallel to $\hat{\theta}$ (Fig. 1c). This is the incompressible limit. In this limit, the slow mode is sometimes called the pseudo-Alfvén mode (Goldreich & Sridhar 1995).

4.2. Theoretical considerations

Here we address the issue of mode coupling in a low β plasma. It is reasonable to suppose that in the limit where $\beta \gg 1$ turbulence for Mach numbers ($M_s = \delta V/a$) less than unity should be largely similar to the exactly incompressible regime. Thus, Lithwick & Goldreich (2001) conjectured that the GS95 relations are applicable to slow and Alfvén modes with the fast modes decoupled. They also mentioned that this relation can carry on for low β plasmas. For $\beta \gg 1$ and $M_s > 1$, we are in the regime of hydrodynamic compressible turbulence for which no theory exists, as far as we know.

⁹In this section, we assume that external mean field is strong (i.e. $V_A > (\delta V)$) but finite, so that $\beta \rightarrow \infty$ means the gas pressure $\bar{P}_g \rightarrow \infty$.

In the diffuse interstellar medium β is typically less than unity. In addition, it is ~ 0.1 or less for molecular clouds. There are a few simple arguments suggesting that MHD theory can be formulated in the regime where the Alfvén Mach number ($\equiv \delta V/V_A$) is less than unity, although this is not a universally accepted assumption. Alfvén modes describe incompressible motions. Arguments in GS95 are suggestive that the coupling of Alfvén to fast and slow modes will be weak. Consequently, we expect that in this regime the Alfvén cascade should follow the GS95 scaling. Moreover the slow waves are likely to evolve passively (Lithwick & Goldreich 2001). For $a \ll V_A$ their nonlinear evolution should be governed by Alfvén modes so that we expect the GS95 scaling for them as well. The phase velocity of Alfvén waves and slow waves depend on a factor of $\cos\theta$ and this enables modulation of the slow waves by the Alfvén ones. However, fast waves do not have this factor and therefore cannot be modulated by the changes of the magnetic field direction associated with Alfvén waves. The coupling between the modes is through the modulation of the local Alfvén velocity and therefore is weak.

For Alfvén Mach number (M_A) larger than unity a shock-type regime is expected. However, generation of magnetic field by turbulence (Cho & Vishniac 2000a) is expected for such a regime. It will make the steady state turbulence approach $M_A \sim 1$.¹⁰ Therefore in Cho & Lazarian (2002a) we consider turbulence in the limit $M_s > 1$, $M_A < 1$, and $\beta < 1$. For these simulations, we mostly used $M_s \sim 2.2$, $M_A \sim 0.7$, and $\beta \sim 0.2$. The Alfvén speed of the mean external field is similar to the rms velocity ($V_A = 1$, $\delta V \sim 0.7$, $a = \sqrt{0.1}$), and we used an isothermal equation of state.

Although the scaling relations presented below are applicable to sub-Alfvénic turbulence, we cautiously speculate that small scales of super-Alfvénic turbulence might follow similar scalings. Boldyrev, Nordlund, & Padoan (2001) obtained energy spectra close to $E(k) \sim k^{-1.74}$ in solenoidally driven super-Alfvénic supersonic turbulence simulations. The spectra are close to the Kolmogorov spectrum ($\sim k^{-5/3}$), rather than shock-dominated spectrum ($\sim k^{-2}$). This result might imply that small scales of super-Alfvénic MHD turbulence can be described by our sub-Alfvénic model presented below, which predicts Kolmogorov-type spectra for Alfvén and slow modes.

4.3. Coupling of MHD modes and Scaling of Alfvén modes

Alfvén modes are not susceptible to collisionless damping (see Spangler 1991; Minter & Spangler 1997 and references therein) that damps slow and fast modes. Therefore, we mainly consider the transfer of energy from Alfvén waves to compressible MHD waves (i.e. to the slow and fast modes).

In Cho & Lazarian (2002a), we carry out simulations to check the strength of the mode-mode coupling. We first obtain a data cube from a driven compressible numerical simulation with

¹⁰We suspect that simulations that show super-Alfvénic turbulence is widely spread in the ISM might not evolve for a long enough time to reach the steady state.

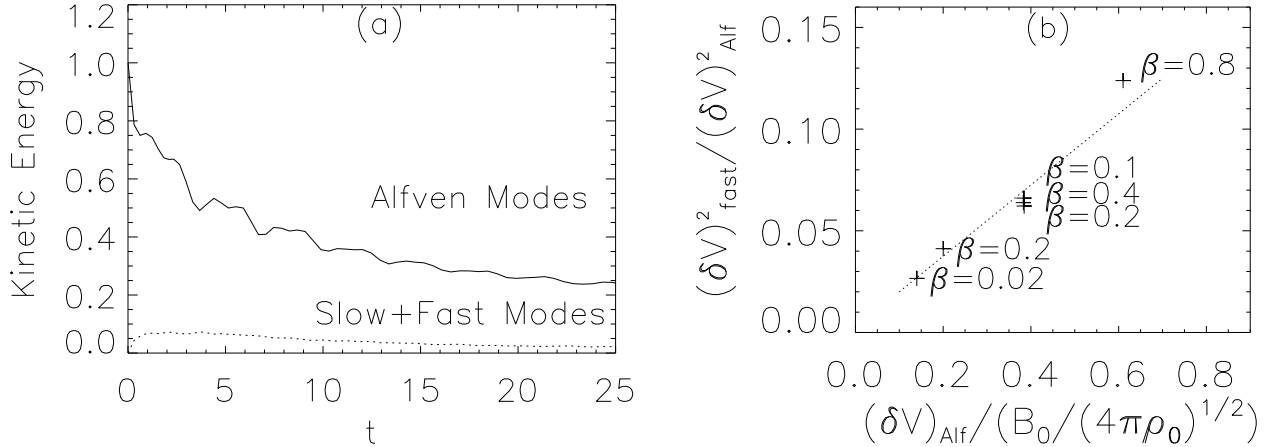


Fig. 3.— (Left) Decay of Alfvénic turbulence. The generation of fast and slow waves is not efficient. $\beta \sim 0.2$, $M_s \sim 3$. (Right) The ratio of $(\delta V)_f^2$ to $(\delta V)_A^2$. The stronger the external field (B_0) is, the more suppressed the coupling is. The ratio is not sensitive to β . From Cho & Lazarian (2002a)

$B_0/\sqrt{4\pi\rho_0} = 1$. Then, after turning off the driving force, we let the turbulence decay. We go through the following procedures before we let the turbulence decay. We first remove slow and fast modes in Fourier space and retain only Alfvén modes. We also change the value of \mathbf{B}_0 preserving its original direction. We use the same constant initial density ρ_0 for all simulations. We assign a new constant initial gas pressure P_g ¹¹. After doing all these procedures, we let the turbulence decay. We repeat the above procedures for different values of B_0 and P_g . Fig. 3a shows the evolution of the kinetic energy of a simulation. The solid line represents the kinetic energy of Alfvén modes. It is clear that Alfvén waves are poorly coupled to the compressible modes, and do not generate them efficiently¹² Therefore, we expect that Alfvén modes will follow the same scaling relation as in the incompressible case. Fig. 3b shows that the coupling gets weaker as B_0 increases:

$$\frac{(\delta V)_f^2}{(\delta V)_A^2} \propto \frac{(\delta V)_A}{B_0}. \quad (14)$$

The ratio of $(\delta V)_s^2$ to $(\delta V)_A^2$ is proportional to $(\delta V)_A^2/B_0^2$.

This marginal coupling is in good agreement with a claim in GS95, as well as earlier numerical studies where the velocity was decomposed into a compressible component \mathbf{v}_C and a solenoidal

¹¹The changes of both B_0 and P_g preserve the Alfvén character of perturbations. In Fourier space, the mean magnetic field (\mathbf{B}_0) is the amplitude of $\mathbf{k} = \mathbf{0}$ component. Alfvén components in Fourier space are for $\mathbf{k} \neq \mathbf{0}$ and their directions are parallel/anti-parallel to $\hat{\xi}_A (= \hat{\mathbf{B}}_0 \times \hat{\mathbf{k}}_\perp)$. The direction of $\hat{\xi}_A$ does not depend on the magnitude of B_0 or P_g .

¹²As correctly pointed out by Zweibel (this volume) there is always residual coupling between Alfvén and compressible modes due to steepening of Alfvén modes. However, this steepening happens on time-scales much longer than the cascading time-scale.

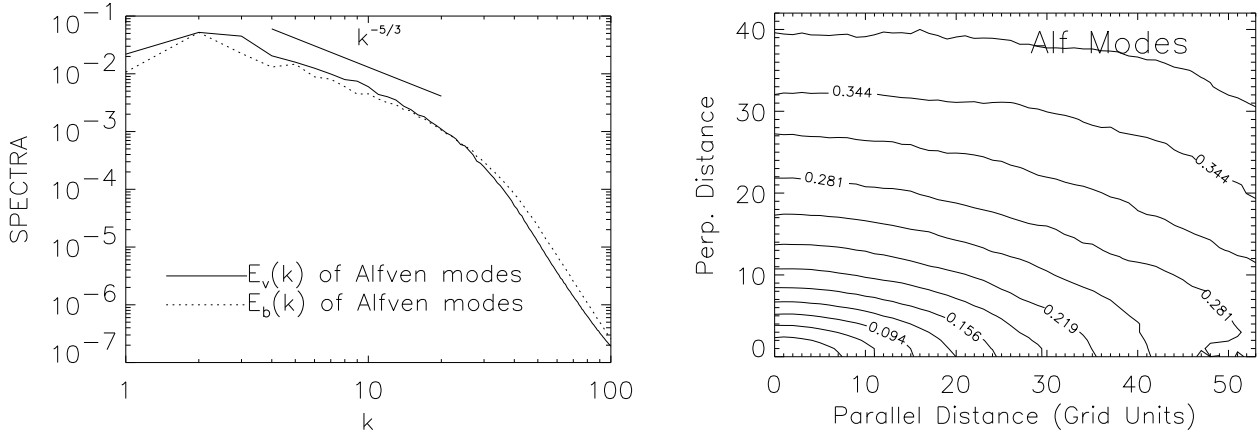


Fig. 4.— (a) Alfvén spectra follow a Kolmogorov-like power law. (b) The second-order structure function ($SF_2 = \langle \mathbf{v}(\mathbf{x} + \mathbf{r}) - \mathbf{v}(\mathbf{x}) \rangle$) for Alfvén velocity shows anisotropy similar to the GS95. Contours represent eddy shapes. From Cho & Lazarian (2002a).

component \mathbf{v}_S . The compressible component is curl-free and parallel to the wave vector \mathbf{k} in Fourier space. The solenoidal component is divergence-free and perpendicular to \mathbf{k} . The ratio $\chi = (\delta V)_C / (\delta V)_S$ is an important parameter that determines the strength of any shock (Passot et al. 1988; Pouquet 1999). Porter, Woodward, & Pouquet (1998) performed a hydrodynamic simulation of decaying turbulence with an initial sonic Mach number of unity and found that χ^2 evolves toward ~ 0.11 . Matthaeus et al. (1996) carried out simulations of decaying weakly compressible MHD turbulence (Zank & Matthaeus 1993) and found that $\chi^2 \sim O(M_s^2)$, where M_s is the sonic Mach number. In Boldyrev et al. (2001) a weak generation of compressible components in solenoidally driven super-Alfvénic supersonic turbulence simulations was obtained.

Fig. 4 shows that the spectrum and the anisotropy of Alfvén waves in this limit are compatible with the GS95 model:

$$\text{Spectrum of Alfvén Modes: } E(k) \propto k_{\perp}^{-5/3}, \quad (15)$$

and scale-dependent anisotropy $k_{\parallel} \propto k_{\perp}^{2/3}$ that is compatible with the GS95 theory.

4.4. Scaling of the slow modes

Slow waves are somewhat similar to pseudo-Alfvén waves (in the incompressible limit). First, the directions of displacement (i.e. ξ_s) of both waves are similar when anisotropy is present. The vector ξ_s is always between $\hat{\theta}$ and $\hat{\mathbf{k}}_{\parallel}$. In Figure 1, we can see that the angle between $\hat{\theta}$ and $\hat{\mathbf{k}}_{\parallel}$ gets smaller when $k_{\parallel} \ll k_{\perp}$. Therefore, when there is anisotropy (i.e. $k_{\parallel} \ll k_{\perp}$), $\hat{\xi}_s$ of a low β plasma becomes similar to that of a high β plasma. Second, the angular dependence in the dispersion relation $c_s \approx a \cos \theta$ is identical to that of pseudo-Alfvén waves (the only difference is that, in slow waves, the sound speed a is present instead of the Alfvén speed V_A).

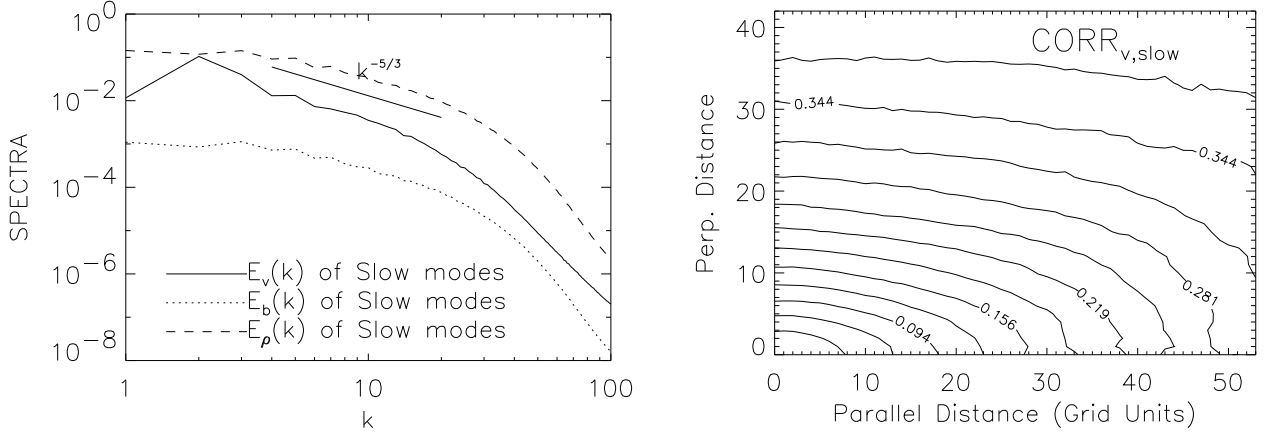


Fig. 5.— (a) Slow spectra also follow a Kolmogorov-like power law. (b) Slow modes show anisotropy similar to the GS95 theory. From Cho & Lazarian (2002a).

Goldreich & Sridhar (1997) argued that the pseudo-Alfvén waves are slaved to the shear-Alfvén (i.e. ordinary Alfvén) waves in the presence of a strong \mathbf{B}_0 , meaning that the energy cascade of pseudo-Alfvén modes is primarily mediated by the shear-Alfvén waves. This is because pseudo-Alfvén waves do not provide efficient shearing motions. Similar arguments are applicable to slow waves in a low β plasma (Cho & Lazarian 2002a) (see also Lithwick & Goldreich 2001 for high- β plasmas). As a result, we conjecture that slow modes follow a scaling similar to the GS95 model (Cho & Lazarian 2002a):

$$\text{Spectrum of Slow Modes: } E^s(k) \propto k_{\perp}^{-5/3}. \quad (16)$$

Fig. 5a shows the spectra of slow modes. For velocity, the slope is close to $-5/3$. Fig. 5b shows the contours of equal second-order structure function (SF_2) of slow velocity, which are compatible with $k_{\parallel} \propto k_{\perp}^{2/3}$ scaling.

In low β plasmas, density fluctuations are dominated by slow waves (Cho & Lazarian 2002a). From the continuity equation $\dot{\rho} = \rho \nabla \cdot \mathbf{v}$

$$\omega \rho_k = \rho_0 \mathbf{k} \cdot \mathbf{v}_k, \quad (17)$$

we have, for slow modes, $(\rho_k)_s \sim \rho_0 (v_k)_s / a$. Hence, this simple argument implies

$$\left(\frac{\delta \rho}{\rho} \right)_s = \frac{(\delta V)_s}{a} \sim M_s, \quad (18)$$

where we assume that $(\delta V)_s \sim (\delta V)_A$ and M_s is the Mach number. On the other hand, only a small amount of magnetic field is produced by the slow waves. Similarly, using the induction equation ($\omega \mathbf{b}_k = \mathbf{k} \times (\mathbf{B}_0 \times \mathbf{v}_k)$), we have

$$\frac{(\delta B)_s}{(\delta V)_s} \sim \frac{a}{B_0} = O(\sqrt{\beta}), \quad (19)$$

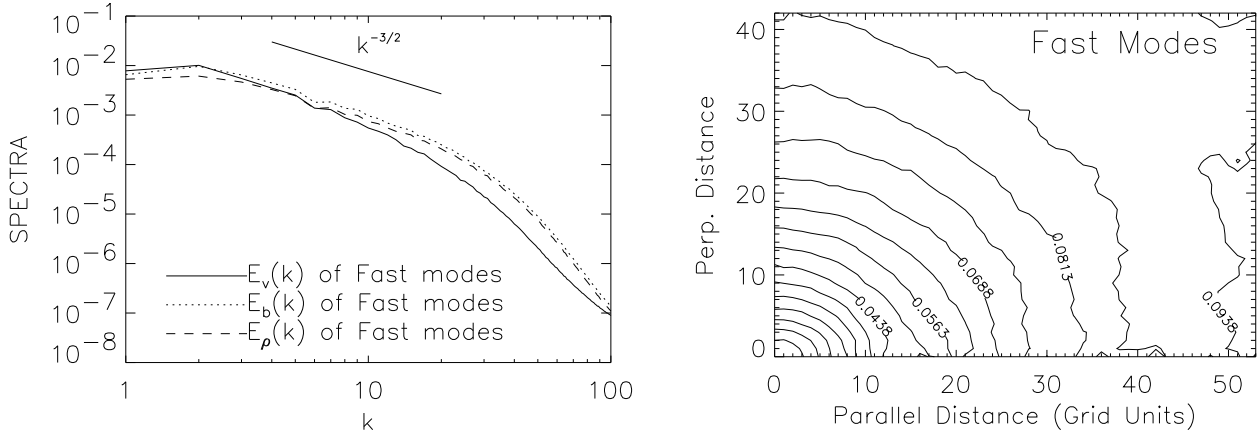


Fig. 6.— (a) The power spectrum of fast waves is compatible with the IK spectrum. (b) The magnetic second-order structure function of fast modes shows isotropy. From Cho & Lazarian (2002a).

which means that equipartition between kinetic and magnetic energy is not guaranteed in low β plasmas. In fact, in Fig. 5a, the power spectrum for density fluctuations has a much larger amplitude than the magnetic field power spectrum. Since density fluctuations are caused mostly by the slow waves and magnetic fluctuation is caused mostly by Alfvén and fast modes, we *do not* expect a strong correlation between density and magnetic field, which agrees with the ISM simulations (Padoan & Nordlund 1999; Ostriker et al. 2001; Vazquez-Semadeni 2002).

4.5. Scaling of the fast modes

Figure 6 shows fast modes are isotropic. The resonance conditions for interacting fast waves are:

$$\omega_1 + \omega_2 = \omega_3, \quad (20)$$

$$\mathbf{k}_1 + \mathbf{k}_2 = \mathbf{k}_3. \quad (21)$$

Since $\omega \propto k$ for the fast modes, the resonance conditions can be met only when all three \mathbf{k} vectors are collinear. This means that the direction of energy cascade is *radial* in Fourier space, and we expect an isotropic distribution of energy in Fourier space.

Using the constancy of energy cascade and uncertainty principle, we can derive an IK-like energy spectrum for fast waves. The constancy of cascade rate reads

$$\frac{v_l^2}{t_{cas}} = \frac{k^3 v_k^2}{t_{cas}} = \text{constant}. \quad (22)$$

On the other hand, t_{cas} can be estimated as

$$t_{cas} \sim \frac{v_k}{(\mathbf{v} \cdot \nabla \mathbf{v})_{\mathbf{k}}} \sim \frac{v_k}{\sum_{\mathbf{p}+\mathbf{q}=\mathbf{k}} k v_p v_q}. \quad (23)$$

If contributions are random, the denominator can be written by the square root of the number of interactions ($\sqrt{\mathcal{N}}$) times strength of individual interactions ($\sim kv_k^2$)¹³. Here we assume locality of interactions: $p \sim q \sim k$. Due to the uncertainty principle, the number of interactions becomes $\mathcal{N} \sim k(\Delta k)^2$, where Δk is the typical transversal (i.e. not radial) separation between two wave vectors \mathbf{p} and \mathbf{q} (with $\mathbf{p} + \mathbf{q} = \mathbf{k}$). Therefore, the denominator of equation (23) is $(k(\Delta k)^2)^{1/2} kv_k^2$. We obtain an independent expression for t_{cas} from the uncertainty principle ($t_{cas}\Delta\omega \sim 1$ with $\Delta\omega \sim \Delta k(\Delta k/k)$). From this and equation (23), we get $t_{cas} \sim t_{cas}^{1/2}/(k^2 v_k)$, which yields

$$t_{cas} \sim 1/k^4 v_k^2. \quad (24)$$

Combining equations (22) and (24), we obtain $v_k^2 \sim k^{-7/2}$, or $E^f(k) \sim k^2 v_k^2 \sim k^{-3/2}$. This is very similar to acoustic turbulence, turbulence caused by interacting sound waves (Zakharov 1967; Zakharov & Sagdeev 1970; L’vov, L’vov, & Pomyalov 2000). Zakharov & Sagdeev (1970) found $E(k) \propto k^{-3/2}$. However, there is debate about the exact scaling of acoustic turbulence. Here we cautiously claim that our numerical results are compatible with the Zakharov & Sagdeev scaling:

$$\text{Spectrum of Fast Modes: } E^f(k) \sim k^{-3/2}. \quad (25)$$

Magnetic field perturbations are mostly affected by fast modes (Cho & Lazarian 2002a) when β is small:

$$\text{Fast: } \frac{(\delta B)_f}{(\delta V)_A} \sim \frac{(\delta V)_f}{(\delta V)_A}, \quad (26)$$

if $(\delta V)_A \sim (\delta V)_s$.

The turbulent cascade of fast modes is expected to be slow and in the absence of collisionless damping they are expected to propagate in turbulent media over distances considerably larger than Alfvén or slow modes. This effect is difficult to observe in numerical simulations with $\Delta B \sim B_0$. A modification of the spectrum in the presence of the collisionless damping is presented in Yan & Lazarian (2002).

5. Implication for Cosmic Ray Propagation

Many astrophysical problems require some knowledge of the scaling properties of turbulence. Therefore we expect a wide range of applications of the established scaling relations. Here we show how recent progress in understanding MHD turbulence affects cosmic ray propagation.

The propagation of cosmic rays is mainly determined by their interactions with electromagnetic fluctuations in interstellar medium. The resonant interaction of cosmic ray particles with MHD

¹³To be exact, the strength of individual interactions is $\sim kv_k^2 \sin \theta$, where θ is the angle between \mathbf{k} and \mathbf{B}_0 . Thus marginal anisotropy is expected. It will be investigated elsewhere.

turbulence has been repeatedly suggested as the main mechanism for scattering and isotropizing cosmic rays. In these analysis it is usually assumed that the turbulence is *isotropic* with a Kolmogorov spectrum (see Schlickeiser & Miller 1998). How should these calculations be modified?

Consider resonance interaction first. Particles get into resonance with MHD perturbations propagating along the magnetic field if the resonant condition is fulfilled, namely, $\omega = k_{\parallel}v\mu + n\Omega$ ($n = \pm 1, 2, \dots$), where ω is the wave frequency, $\Omega = \Omega_0/\gamma$ is the gyrofrequency of relativistic particle, $\mu = \cos \alpha$, where α is the pitch angle of particles. In other words, resonant interaction between a particle and the transverse electric field of a wave occurs when the Doppler shifted frequency of the wave in the particle's guiding center rest frame $\omega_{gc} = \omega - k_{\parallel}v\mu$ is a multiple of the particle gyrofrequency.

For cosmic rays, $k_{\parallel}v_{\parallel} \gg \omega$ so the slow variation of the magnetic field with time can be neglected. Thus the resonant condition is simply $k_{\parallel}v\mu + n\Omega = 0$. From this resonance condition, we know that the most important interaction occurs at $k_{\parallel} = k_{res} = \Omega/v_{\parallel}$.

It is intuitively clear that resonant interaction of particles in isotropic and anisotropic turbulence should be different. Chandran (2001) obtained strong suppression of scattering by Alfvénic turbulence when he treated turbulence anisotropies in the spirit of Goldreich-Sridhar model of incompressible turbulence. His treatment was improved in Yan & Lazarian (2002, henceforth YL02) who used a more rigorous rather than an ad hoc description of magnetic field statistics and took into account compressibility of turbulence. In our description we shall follow YL02 treatment of the problem.

We employ quasi-linear theory (QLT) to obtain our estimates. QLT has been proved to be a useful tool in spite of its intrinsic limitations (Chandran 2001; Schlickeiser & Miller 1998; Miller 1997). For moderate energy cosmic rays, the corresponding resonant scales are much smaller than the injection scale. Therefore the fluctuation on the resonant scale $\delta B \ll B_0$ even if they are comparable at the injection scale. QLT disregards diffusion of cosmic rays that follow wandering magnetic field lines (Jokipii 1966) and this diffusion should be accounted separately. Obtained by applying the QLT to the collisionless Boltzmann-Vlasov equation, the Fokker-Planck equation is generally used to describe the evolution of the gyrophase-average distribution function f ,

$$\frac{\partial f}{\partial t} = \frac{\partial}{\partial \mu} \left(D_{\mu\mu} \frac{\partial f}{\partial \mu} + D_{\mu p} \frac{\partial f}{\partial p} \right) + \frac{1}{p^2} \frac{\partial}{\partial p} \left[p^2 \left(D_{\mu p} \frac{\partial f}{\partial \mu} + D_{pp} \frac{\partial f}{\partial p} \right) \right],$$

where p is particle momentum. The Fokker-Planck coefficients $D_{\mu\mu}, D_{\mu p}, D_{pp}$ are the fundamental physical parameter for measuring the stochastic interactions, which are determined by the electromagnetic fluctuations (Schlickeiser & Achatz 1993). From Ohm's Law $\mathbf{E}(\mathbf{k}) = -(1/c)\mathbf{v}(\mathbf{k}) \times \mathbf{B}_0$, we can get the electromagnetic fluctuations from correlation tensors of magnetic and velocity fluctuations C_{ij}, K_{ij} . Here,

$$\begin{aligned} \langle B_i(\mathbf{k})B_j^*(\mathbf{k}') \rangle / B_0^2 &= \delta(\mathbf{k} - \mathbf{k}')M_{ij}(\mathbf{k}), \\ \langle v_i(\mathbf{k})B_j^*(\mathbf{k}') \rangle / V_A B_0 &= \delta(\mathbf{k} - \mathbf{k}')C_{ij}(\mathbf{k}), \end{aligned}$$

$$\langle v_i(\mathbf{k})v_j^*(\mathbf{k}') \rangle / V_A^2 = \delta(\mathbf{k} - \mathbf{k}')K_{ij}(\mathbf{k}). \quad (27)$$

For Alfven modes, Cho, Lazarian and Vishniac (2002) obtained

$$K_{ij}(\mathbf{k}) = C_a I_{ij} k_{\perp}^{-10/3} \exp(-L^{1/3} k_{\parallel} / k_{\perp}^{2/3}), \quad (28)$$

where $I_{ij} = \{\delta_{ij} - k_i k_j / k_{\perp}^2\}$ is a 2D matrix in x-y plane, k_{\parallel} is the wave vector along the local mean magnetic field, k_{\perp} is the wave vector perpendicular to the magnetic field and the normalization constant $C_a = L^{-1/3} / 12\pi$. We assume that for the Alfven modes $M_{ij} = K_{ij}$, $C_{ij} = \sigma M_{ij}$ where the fractional helicity $-1 < \sigma < 1$ is independent of \mathbf{k} (Chandran 2001). According to Cho & Lazarian (2002a), fast modes are isotropic and have one dimensional spectrum $E(k) \propto k^{-3/2}$. In low β medium, the velocity fluctuations are always perpendicular to \mathbf{B}_0 for all \mathbf{k} , while the magnetic fluctuations are perpendicular to \mathbf{k} . Thus K_{ij} , M_{ij} of fast modes are not equal,

$$\begin{bmatrix} M_{ij}(\mathbf{k}) \\ C_{ij}(\mathbf{k}) \\ K_{ij}(\mathbf{k}) \end{bmatrix} = \frac{L^{-1/2}}{8\pi} J_{ij} k^{-7/2} \begin{bmatrix} \cos^2 \theta \\ \sigma \cos^2 \theta \\ 1 \end{bmatrix}, \quad (29)$$

where $J_{ij} = k_i k_j / k_{\perp}^2$ is also a 2D tensor in $x - y$ plane¹⁴. In high β medium, the velocity fluctuations are radial, i.e., along the direction of \mathbf{k} . Fast modes in this regime are essentially sound waves compressing magnetic field (GS95; Cho & Lazarian, in preparation). The compression of magnetic field depends on plasma β . The corresponding tensors are

$$\begin{bmatrix} M_{ij}(\mathbf{k}) \\ C_{ij}(\mathbf{k}) \\ K_{ij}(\mathbf{k}) \end{bmatrix} = \frac{L^{-1/2}}{8\pi} J_{ij} k^{-7/2} \begin{bmatrix} \cos^2 \theta \sin^2 \theta / \beta^{3/2} \\ 0 \\ \sin^2 \theta \end{bmatrix}. \quad (30)$$

Adopting the approach in Schlickeiser & Achatz (1993), we can obtain the Fokker-Planck coefficients in the lowest order approximation of V_A/c ,

$$\begin{aligned} \begin{bmatrix} D_{\mu\mu} \\ D_{\mu p} \\ D_{pp} \end{bmatrix} &= \frac{\Omega^2(1 - \mu^2)}{2B_0^2} \begin{bmatrix} 1 \\ mc \\ m^2 c^2 \end{bmatrix} \mathcal{R}e \sum_{n=-\infty}^{n=\infty} \int_{k_{min}}^{k_{max}} dk^3 \\ &\int_0^{\infty} dt e^{-i(k_{\parallel} v_{\parallel} - \omega + n\Omega)t} \left\{ J_{n+1}^2 \left(\frac{k_{\perp} v_{\perp}}{\Omega} \right) \begin{bmatrix} P_{\mathcal{R}\mathcal{R}}(\mathbf{k}) \\ T_{\mathcal{R}\mathcal{R}}(\mathbf{k}) \\ R_{\mathcal{R}\mathcal{R}}(\mathbf{k}) \end{bmatrix} \right. \\ &+ J_{n-1}^2 \left(\frac{k_{\perp} v_{\perp}}{\Omega} \right) \begin{bmatrix} P_{\mathcal{L}\mathcal{L}}(\mathbf{k}) \\ -T_{\mathcal{L}\mathcal{L}}(\mathbf{k}) \\ R_{\mathcal{L}\mathcal{L}}(\mathbf{k}) \end{bmatrix} + J_{n+1} \left(\frac{k_{\perp} v_{\perp}}{\Omega} \right) J_{n-1} \left(\frac{k_{\perp} v_{\perp}}{\Omega} \right) \\ &\left. \left[e^{i2\phi} \begin{bmatrix} -P_{\mathcal{R}\mathcal{L}}(\mathbf{k}) \\ T_{\mathcal{R}\mathcal{L}}(\mathbf{k}) \\ R_{\mathcal{R}\mathcal{L}}(\mathbf{k}) \end{bmatrix} + e^{-i2\phi} \begin{bmatrix} -P_{\mathcal{L}\mathcal{R}}(\mathbf{k}) \\ -T_{\mathcal{L}\mathcal{R}}(\mathbf{k}) \\ R_{\mathcal{L}\mathcal{R}}(\mathbf{k}) \end{bmatrix} \right] \right\} \quad (31) \end{aligned}$$

¹⁴This tensor is different from that in Schlickeiser & Miller (1998). The fact that the fluctuations $\delta\mathbf{B}$ in fast modes are in the \mathbf{k} - \mathbf{B} plane place another constrain on the tensor so that the term δ_{ij} doesn't exist.

where $k_{min} = L^{-1}$, $k_{max} = \Omega_0/v_{th}$ corresponds to the dissipation scale, $m = \gamma m_H$ is the relativistic mass of the proton, v_{\perp} is the particle's velocity component perpendicular to \mathbf{B}_0 , $\phi = \arctan(k_y/k_x)$, $\mathcal{L}, \mathcal{R} = (x \pm iy)/\sqrt{2}$ represent left and right hand polarization.

5.1. Scattering by Alfvénic turbulence

Noticing that the integrand for small k_{\perp} is substantially suppressed by the exponent in the anisotropic tensor (see Eq. (28)) so that the large scale contribution is not important, we can simply use the asymptotic form of Bessel function for large argument. Then if the pitch angle α satisfies $\sin \alpha \ll \gamma v_{th}/v$, we can derive the analytical result for anisotropic turbulence (YL02),

$$\begin{bmatrix} D_{\mu\mu} \\ D_{\mu p} \\ D_{pp} \end{bmatrix} = \frac{v^{2.5} \cos \alpha^{5.5}}{24\pi\Omega^{1.5} L^{17/6} \sin \alpha} \Gamma[6.5, k_{max}^{2/3} k_{res} L^{1/3}] \begin{bmatrix} 1 \\ \sigma m V_A \\ m^2 V_A^2 \end{bmatrix}, \quad (32)$$

where L is the injection scale, $k_{max} = \Omega_0/v_{th}$ corresponds to the dissipation scale, $\Gamma[a, z]$ represents the incomplete gamma function. This result is different from Chandran's by a factor of *Gamma*.

The scattering frequency $\nu = 2D_{\mu\mu}/(1 - \mu^2)$ is plotted for different models in Fig.(7a). It is clear that anisotropy suppresses scattering. Although our results are ~ 3 orders larger than those obtained in Chandran (2001) using an *ad hoc* tensor with a step function¹⁵, they are still much smaller than the estimates for isotropic model. Unless we consider very high energy CRs ($\geq 10^8 GeV$) with corresponding Larmor radius comparable to the injection scale at which the Alfvénic turbulence is still isotropic, we can neglect scattering by the Alfvénic turbulence. What is the alternative way to scatter cosmic rays?

5.2. Scattering by fast modes

For compressible modes we discuss two types of resonant interaction: gyroresonance and transit-time damping; the latter requires longitudinal motions. The contribution from slow modes is not larger than that by Alfvén modes since the slow modes have the similar anisotropies and scalings. More promising are fast modes, which are isotropic (Cho & Lazarian 2002a). However, fast modes are subject to collisionless damping which suppresses scattering. The damping rate $\gamma_d = \tau_d^{-1}$ for the low β case (Ginzburg 1961) is

$$\gamma_d = \frac{\sqrt{\pi\beta}}{4} V_A k \frac{\sin^2 \theta}{\cos \theta} \times \left[\sqrt{\frac{m_e}{m_H}} \exp\left(-\frac{m_e}{m_H \beta \cos^2 \theta}\right) \right]$$

¹⁵We counted only the resonant term in Chandran (2001). The nonresonant term is spurious as noted by Chandran (2001)

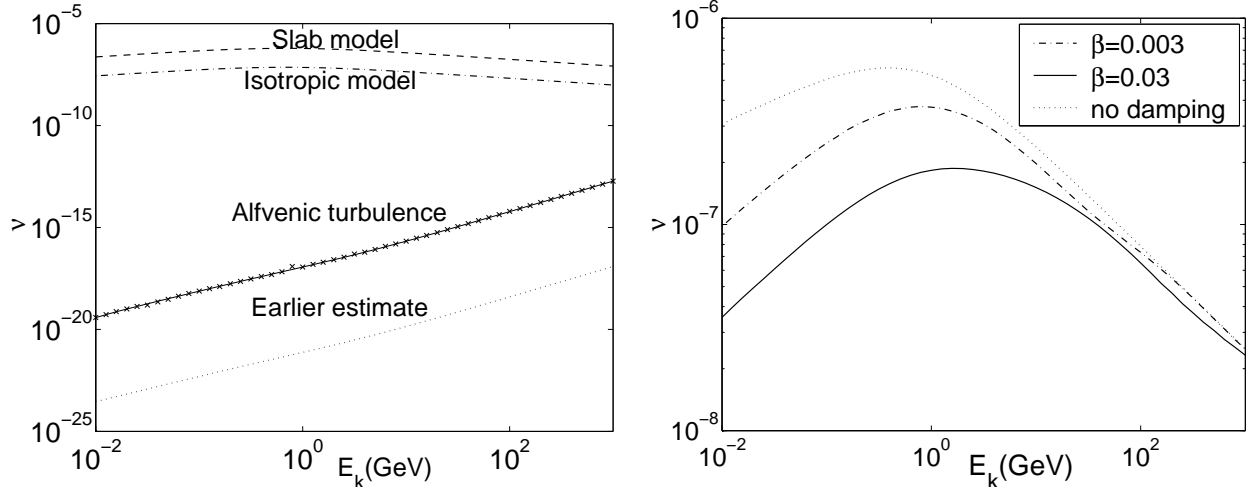


Fig. 7.— The scattering frequency ν vs. the kinetic energy E_k of cosmic rays (a) by Alfvénic turbulence, (b) by fast modes. In (a), the dash-dot line refers to the scattering frequency for isotropic turbulence. The ‘x’ represents our numerical result for anisotropic turbulence, the solid line is our analytical result from Eq. (32). Also plotted (dashed line) is the previous result for anisotropic turbulence in Chandran (2001). In (b), the dashed line represents the scattering by fast modes immune from damping, the solid and dashdot line are the results taking into account collisionless damping. (From Yan & Lazarian 2002)

$$+ 5 \exp\left(-\frac{1}{\beta \cos^2 \theta}\right)], \quad (33)$$

where m_e is the electron mass. We see that the damping increases with β for low β medium. According to CL02, fast modes cascade over time scales $\tau_{fk} = \tau_k \times V_A/v_k = (k \times k_{min})^{-1/2} \times V_A/V^2$, where $\tau_k = kv_k$ is the eddy turn-over time, V is the turbulence velocity at the injection scale.

Consider gyroresonance scattering in the presence of collisionless damping, the cutoff of fast modes corresponds to the scale where $\tau_{fk}\gamma_d \simeq 1$ and this defines the cutoff scale k_c^{-1} . As we see from Eq.(33), the damping increases with θ .

Using the tensors given in Eq.(29) we obtain the corresponding Fokker-Planck coefficients for the CRs interacting with fast modes by integrating Eq.(31) from k_{min} to k_c (see Fig.(7b)). When k_c^{-1} is less than r_L , the results of integration for damped and undamped turbulence coincides. Since the k_c decreases with β , the scattering frequency decreases with β .

Since our scattering frequency is related to the spatial diffusion coefficient by $D \propto \int_0^1 d\mu(1 - \mu^2)/\nu$ (see Schlickeiser & Miller 1998; Seo & Ptuskin 1994), and the escape length by $X_e \propto 1/D$ (Seo & Ptuskin 1994; Berezhinskii et al. 1990), X_e has the same energy dependence as the scattering frequency ν . It has been suggested that to reproduce the observed B/C and other secondary/primary ratios requires a turn-off in the CRs’ path length distribution around $E_k \simeq 1\text{GeV}$ (Webber 1993; Garcia et al. 1987). The scattering frequency, according to Eq.(31), increases with

Larmor frequency Ω_0/γ and the resonant scale $k_{res}^{-1} \sim r_L$, which increase with proton energy E_k . For $E_k < m_p c^2 \simeq 1\text{GeV}$, γ changes very slowly with E_k , so the scale dependence is dominant, while for $E_k > 1\text{GeV}$, γ goes nearly linearly with E_k so that the scattering frequency decreases due to the Ω_0/γ dependence which changes more rapidly. Incidentally, this corresponds to the energy of the observed peak of secondary to primary ratio B/C. More important, for high energy CRs ($E_K > 10\text{GeV}$, the scattering by fast modes in low β plasma produces a steeper spectrum of $X_e \propto E^{-\delta}$, $\delta = 0.52$ than Kolmogorov model ($\delta = 0.33$), which is favored by observations (Swordy 2001).

Adopting the tensors given in Eq.(30) and damping from Foote & Kulsrud (1979), we calculated the scattering frequency of CRs in high β medium. Our results show that the fast modes still dominate the CRs' scattering in spite of the fact that the scattering frequency is 2 orders (for $\beta \simeq 300$) smaller than that in low β case. In such a medium, the turnoff of the scattering frequency appears at $E_k \simeq 0.4\text{GeV}$.

5.3. Cosmic ray self-confinement by streaming instability

When cosmic rays stream at a velocity much larger than Alfvén velocity, they can excite resonant MHD waves which in turn scatter themselves. This is so called streaming instability. It was claimed that the instability can provide confinement for cosmic rays with energy less than 100GeV (Cesarsky 1980). However, this is calculated in an ideal regime, i.e., there is no background MHD turbulence. Only ambipolar collisional damping is involved. In other words, the self-excited waves will not be damped in fully ionized gas, which is not true for turbulent medium. Here we shall reconsider in turbulent ISM how this instability would affect cosmic ray transport, whether it is still an effective mechanism. Fast turbulent damping of Alfvénic modes is expected to mitigate the instability.

In the moving frame in which cosmic rays are isotropic, the growth rate of the waves of wave number k is given by (Longair 1997)

$$G(k) = \Omega \frac{N(\geq E)}{n_p} \left(-1 + \frac{v}{V_A}\right), \quad (34)$$

where $n \geq E$ is the number density of cosmic rays with energy $\geq E$ which resonants with the wave, i.e., $v(E) = \Omega/k.n_p$ is the number density of charged particles in the medium. If taking the energy spectrum of cosmic ray particles $n(E) \propto E^x$ ($x \sim 2.7$) as measured at the Earth (Longair 1997), $n(E) \simeq 0.25 \times 10^{-10} \text{ cm}^{-3}$ (using the same parameter as given in Figure 7), so that

$$G(k) = 5.4 \times 10^{-11} \left(-1 + \frac{v}{V_A}\right) \left(\frac{E}{\text{Gev}}\right)^{-1.7} = 1.1 \times 10^{-7} \left(\frac{E}{\text{Gev}}\right)^{-1.7} s^{-1}, \quad (35)$$

while the damping rate for turbulent wave with $k = \Omega/v(E)$ is

$$kV_A = 1.1 \times 10^{-6} \left(\frac{E}{\text{GeV}} \right)^{-1/2} s^{-1}. \quad (36)$$

Comparing Eq. (35) and (36), we see clearly that the streaming instability is only applicable for particles with energy 0.15GeV, which is less than the energy of most cosmic ray particles. So we don't think self-confinement mechanism works as proposed by other authors before. Thus the gyroresonance with the fast modes is the principle mechanism for scattering cosmic rays. This demands a substantial revision of cosmic ray acceleration/propagation theories that will be done elsewhere.

6. Summary

Recently there have been significant advances in the field of compressible MHD turbulence:

1. Simulations of compressible MHD turbulence show that there is a weak coupling between Alfvén waves and compressible MHD waves and that the Alfvén modes follow the Goldreich-Sridhar scaling. Fast modes, however, decouple and exhibit isotropy.
2. Scattering of cosmic rays by Alfvénic modes is suppressed and therefore the scattering by fast modes is the dominant process provided that turbulent energy is injected at large scales.
3. The scattering frequency by fast modes depends on collisionless damping and therefore on plasma β .
4. The streaming instability of cosmic rays is mitigated or suppressed due to a rapid turbulent decay of magnetic fluctuations in the presence of background turbulence.

Acknowledgments: We acknowledge the support of the NSF through grant AST-0125544. This work was partially supported by National Computational Science Alliance under AST000010N and utilized the NCSA SGI/CRAY Origin2000.

REFERENCES

- Armstrong, J. W., Rickett, B. J., & Spangler, S. R. 1995, ApJ, 443, 209
- Baccigalupi, C., Burigana, C., Perrotta, F., De Zotti, G., La Porta, L., Maino, D., Maris, M., & Paladini, R. 2001, A&A, 8
- Berezinskii, V., Bulanov, S., Dogiel, S., Ginzburg, V. & Ptuskin, V., *Astrophysics of Cosmic Rays* (North-Holland, New York, 1990)
- Biskamp, D. 1993, *Nonlinear Magnetohydrodynamics* (Cambridge: Cambridge University Press)

- Boldyrev, S. 2002, ApJ, 569, 841
- Boldyrev, S., Nordlund, A., & Padoan, P. 2001, preprint, astro-ph/0111345
- Brio, M. & Wu, C. 1988, J. Comput. Phys., 75, 500
- Cesarsky, C. 1980, Annu. Rev. Astro. Astrophys., 18, 289
- Chandran, B. 2001, Phys. Rev. Lett., 85, 4656
- Cho, J. & Lazarian, A. 2002a, Phys. Rev. Lett., 88, 245001 (CL02)
- . 2002b, ApJ, 575, L63
- Cho, J., Lazarian, A., & Vishniac, E. T. 2002, ApJ, 564, 291
- Cho, J. & Vishniac, E. T. 2000a, ApJ, 538, 217
- Cho, J. & Vishniac, E. T. 2000b, ApJ, 539, 273
- Deshpande, A. A. 2000, MNRAS, 317, 199
- Deshpande, A. A., Dwarakanath, K. S., & Goss, W. M. 2000, ApJ, 543, 227
- Dickman, R. L. 1985, in Protostars and Planets II, ed. D. C. Black & M. S. Mathews (Tucson: Univ. Arizona Press), 150
- Draine, B. T. 1985, in Protostars and Planets II, ed. D. C. Black & M. S. Mathews (Tucson: Univ. Arizona Press), 621
- Falgarone, E. & Puget, J. L. 1995, A&A, 293, 840
- Foote, E.A. & Kulsrud, R.M. 1979, Astrophys. J., 233, 302
- Fosalba, P., Lazarian, A., Prunet, S., & Tauber, J. A. 2002, ApJ, 564, 762
- Garcia Munoz, M. Simpson, J.A., Guzik, T.G., Wefel, J.F. & Margolis, S.H. 1987, Astrophys. J. Supp., 64, 269
- Giardino, G., Banday, A. J., Fosalba, P., Górski, K. M., Jonas, J. L., O’Mullane, W., & Tauber, J. 2001, A&A, 371, 708
- Giardino, G., Banday, A. J., Górski, K. M., Bennett, K., Jonas, J. L., & Tauber, J. 2002, A&A, 387, 82
- Ginzburg, V. I. 1961, *Propagation of Electromagnetic Waves in Plasma* (New York: Gordon & Breach)
- Goldreich, P. & Sridhar, H. 1995, ApJ, 438, 763
- . 1997, ApJ, 485, 680
- Goldstein, M. L. & Roberts, D. A. 1995, Annu. Rev. Astro. Astrophys., 33, 283
- Goodman, J. & Narayan, R. 1985, MNRAS, 214, 519
- Green, D. A. 1993, MNRAS, 262, 328
- Higdon, J. C. 1984, ApJ, 285, 109

- Horbury, T. S. 1999, in *Plasma Turbulence and Energetic particles in Astrophysics*, ed. M. Ostrowski & R. Schlickeiser (Cracow, Poland: Obserwatorium Astronomiczne, Uniwersytet Jagiellonski), 28
- Horbury, T. S. & Balogh, A. 1997, *Nonlin. Proc. Geophys.*, 4, 185
- Iroshnikov, P. 1963, *Astron. Zh.*, 40, 742 (English: *Sov. Astron.* **7**, 566 (1964))
- Jokipii, J. R. 1966, *ApJ*, 146, 480
- Kampé de Fériet, J. 1955, in *Gas Dynamics of Cosmic Clouds*, IAU Sympo. No. 2 (Amsterdam: North-Holland Pub. Co.), 134
- Kaplan, S. A. & Pickelner, S. B. 1970, *The Interstellar Medium* (Cambridge: Harvard Univ. Press)
- Klein, L., Bruno, R., Bavassano, B., & Rosenbauer, H. 1993, *J. Geophys Res.*, 98, 17461
- Klessen, R. S. 2001, in *Origins of stars and planets: The VLT view*, astro-ph/0106332
- Kolmogorov, A. 1941, *Dokl. Akad. Nauk SSSR*, 31, 538
- Kota, J. & Jokipii, J. R. 2000, *ApJ*, 531, 1067
- Kraichnan, R. 1965, *Phys. Fluids*, 8, 1385
- Kusaka, T., Nakano, T., & Hayashi, C. 1970, *Prog. Theor. Phys.*, 44, 1580
- Larson, R. B. 1981, *MNRAS*, 194, 809
- Lazarian, A. 1995, *A&A*, 293, 507
- Lazarian, A. 1999a, in *Interstellar Turbulence*, ed. J. Franco & A. Carraminana (Cambridge Univ. Press), 95 (astro-ph/9804024)
- Lazarian, A. 1999b, in *Plasma Turbulence and Energetic Particles in Astrophysics*, ed. M. Ostrowski & R. Schlickeiser (Cracow, Poland: Obserwatorium Astronomiczne, Uniwersytet Jagiellonski), 28 (astro-ph/0001001)
- Lazarian, A. 2000, in *ASP, Vol. 215, Cosmic Evolution and Galaxy Formation*, ed. J. Franco, E. Terlevich, O. Lopez-Cruz, & I. Aretxaga (Astron. Soc. Pacific), 69 (astro-ph/0003414)
- Lazarian, A., Goodman, A., & Myers, P. 1997, *ApJ*, 490, 273
- Lazarian, A. & Pogosyan, D. 2000, *ApJ*, 537, 720
- . 2002, in preparation
- Lazarian, A., Pogosyan, D., & Esquivel, A. 2002, in *Seeing Through the Dust*, ed. R. Taylor, T. Landecker, & A. Willis, *ASP Conf. Series (ASP)*, in press (astro-ph/0112368) (LPE02)
- Lazarian, A., Pogosyan, D., Vazquez-Semadeni, E., & Pichardo, B. 2001, *ApJ*, 555, 130
- Lazarian, A. & Prunet, S. 2002, in *AIP Conf. Proc., Vol. 609, Astrophysical Polarized Backgrounds*, ed. S. Cecchini, S. Cortiglioni, R. Sault, & C. Sbarra (Melville, NY: AIP), 32 (astro-ph/0111214)
- Lazarian, A. & Shutenkov, V. R. 1990, *Sov. Astron. Lett.*, 16, 297

- Lazarian, A. & Yan, H. 2002, ApJ, 566, L105
- Leamon, R. J., Smith, C. W., Ness, N. F., & Matthaeus, W. H. 1998, J. Geophys Res., 103, 4775
- Lesieur, M. 1990, *Turbulence In Fluids* (Dordrecht: Kluwer)
- Lithwick, Y. & Goldreich, P. 2001, ApJ, 562, 279
- Longair, M.S. 1997, *High Energy Astrophysics* (Cambridge University Press)
- L’vov, V. S., L’vov, Y. V., & Pomyalov, A. 2000, Phys. Rev. E, 61, 2586
- Mac Low, M. 1998, Phys. Rev. Lett., 80, 2754
- Matthaeus, W. M., Ghosh, S., Oughton, S., & Roberts, D. A. 1996, J. Geophys Res., 101, 7619
- Matthaeus, W. M., Oughton, S., Ghosh, S., & Hossain, M. 1998, Phys. Rev. Lett., 81, 2056
- Miller, J.A. 1997, ApJ, 491, 939
- Minter, A. & Spangler, S. 1997, ApJ, 485, 182
- Monin, A. S. & Yaglom, A. A. 1975, *Statistical Fluid Mechanics: Mechanics of Turbulence*, Vol. 2 (Cambridge: MIT Press)
- Montgomery, D. C. & Matthaeus, W. H. 1995, ApJ, 447, 706
- Montgomery, D. C. & Turner, L. 1981, Phys. Fluids, 24, 825
- Munch, G. 1958, Rev. Mod. Phys., 30, 1035
- Narayan, R. & Goodman, J. 1989, MNRAS, 238, 963
- Ossenkopf, V. 1993, A&A, 280, 617
- Ostriker, E. C., Gammie, C. F., & Stone, J. M. 1999, ApJ, 513, 259
- Ostriker, E. C., Stone, J. M., & Gammie, C. F. 2001, ApJ, 546, 980
- Padoan, P., Goodman, A., Draine, B. T., Juvela, M., Nordlund, A., & Rognvaldsson, O. 2001, ApJ, 559, 1005
- Padoan, P. & Nordlund, A. 1999, ApJ, 526, 279
- Parker, E. N. 1979, *Cosmical magnetic fields: Their origin and their activity* (New York: Oxford University Press)
- Passot, T., Pouquet, A., & Woodward, P. 1988, A&A, 197, 228
- Passot, T., Vazquez-Semadeni, E., & Pouquet, A. 1995, ApJ, 455, 536
- Porter, D., Woodward, P., & Pouquet, A. 1998, Phys. Fluids, 10, 237
- Pouquet, A. 1999, in *Interstellar Turbulence*, ed. J. Franco & A. Carraminana (Cambridge Univ. Press), 87
- Ryu, D. & Jones, T. W. 1995, ApJ, 442, 228
- Scalo, J. M. 1987, in *Interstellar Processes*, ed. D. J. Hollenbach & H. A. Thronson (Dordrecht: Reidel), 349

- Schlickeiser, R. & Achatz, U. 1993, *J. Plasma Phys.*, 49, 63
- Schlickeiser, R. & Miller, J. A. 1998, *ApJ*, 492, 352
- Seo, E. S. & Ptuskin, V. S. 1994, *ApJ*, 431, 705
- Shebalin, J. V., Matthaeus, W. H., & Montgomery, D. C. 1983, *J. Plasma Phys.*, 29, 525
- Simonetti, J. H. 1992, *ApJ*, 386, 170
- Simonetti, J. H. & Cordes, J. M. 1988, in *AIP Conf. Proc.*, Vol. 174, Radio wave scattering in the interstellar medium, ed. J. M. Cordes, B. J. Rickett, & D. C. Backer (New York: AIP), 134
- Spangler, S. R. 1991, *ApJ*, 376, 540
- Spangler, S. R. & Gwinn, C. R. 1990, *ApJ*, 353, L29
- Sridhar, S. & Goldreich, P. 1994, *ApJ*, 432, 612
- Stanimirovic, S. & Lazarian, A. 2001, *ApJ*, 551, L53
- Stone, J. M., Ostriker, E. C., & Gammie, C. F. 1998, *ApJ*, 508, L99
- Swordy, S. P., 2001, *Space Science Rev.*, 99, 85
- Vazquez-Semadeni, E. 2002, in *Seeing Through the Dust*, ed. R. Taylor, T. Landecker, & A. Willis (San Francisco: ASP) (astro-ph/0201072)
- Vazquez-Semadeni, E., Passot, T., & Pouquet, A. 1995, *ApJ*, 441, 702
- . 1996, *ApJ*, 473, 881
- Volk, H. J., Jones, F. C., Morfill, G. E., & Roser, S. 1980, *A&A*, 85, 316
- von Horner, S. 1951, *Zs.F. Ap.*, 30, 17
- Warhaft, Z. 2000, *Annu. Rev. Fluid Mech.*, 32, 203
- Webber, W. R. 1993, *Astrophys. J.*, 402, 188
- Weidenschilling, S. J. & Ruzmaikina, T. V. 1994, *ApJ*, 430, 713
- Wilson, O. C., Munch, G., Flather, E. M., & Coffeen, M. F. 1959, *ApJS*, 4, 199
- Yan, H. & Lazarian, A. 2002, *Phys. Rev. Lett.*, submitted, astro-ph/0205285 (YL02)
- Zakharov, V. E. 1967, *Sov. Phys. JETP*, 24, 455
- Zakharov, V. E. & Sagdeev, A. 1970, *Sov. Phys. Dokl.*, 15, 439
- Zank, G. P. & Matthaeus, W. H. 1993, *Phys. Fluids A*, 5, 257